

## TOPOGRAPHIC EFFECTS ON CONVECTION IN A ROTATING, STRATIFIED FLUID

Michael J. Coates

Department of Environmental Engineering and Centre for Water Research  
University of Western Australia  
Nedlands, Western Australia, 6907

Gregory N. Ivey

Department of Environmental Engineering and Centre for Water Research  
University of Western Australia  
Nedlands, Western Australia, 6907

### ABSTRACT

We describe some preliminary experiments designed to model aspects of oceanic shelf convection in which dense water is formed by cooling over the shallow, stratified shelf waters. A radial barrier is placed across the centre of a heated circular plate in a rotating tank to simulate a semi-circular cooled region adjacent to the coast. If the Rossby radius  $L_R$  is smaller than the shelf width, a rim current will form at the edge of the semi-circular convecting region. This current subsequently becomes unstable and a number of baroclinic eddies form which promote lateral mixing between the heated and ambient fluids. The magnitude of the rim current and the number of eddies generated agree with earlier results obtained in the absence of the barrier. On the other hand, when the Rossby radius is large compared with the shelf width, the formation of the eddies is suppressed, resulting in rather different exchange mechanisms between shelf and surrounding seas. Thus, the ratio  $\bar{W}/L_R$  of the mean width of the continental shelf to the Rossby radius is crucial in the description of shelf convection, with the transition between regimes occurring at  $\bar{W}/L_R \approx 1$ .

### INTRODUCTION

Deep convection occurs when the surface water density is increased by strong cooling across the air-sea interface, with possible augmentation of the density anomaly by very dense brine formed during ice formation (e.g. Warren 1981). Deep convection is important because of its role in the transport of surface water to deeper levels, and consequently, it affects the overturning rates and residence times of the deeper waters, as well as being of importance in a number of environmental and climatic effects, such as the oceanic heat budget and the rate of uptake of  $\text{CO}_2$ , for example (Hay 1993). The deep convection which occurs in the open ocean, remote from

any coastal boundaries, has received the most attention in the literature, but shelf convection is likely to be the more important process in replenishing the deep ocean waters (e.g. Price and Baringer 1994). Here, the exchange of fluid across the open ocean-shelf boundary may have further environmental consequences in influencing the fluxes of nutrients and particulate matter onto and off the shelf, with global significance for the productivity of the shelf waters (e.g. Walsh 1991). In addition, shelf convection is not just confined to a few high latitude locations, as is the case for open ocean convection. However, as Huthnance (1994) points out in his recent review, the contribution of convectively driven processes to the exchange between shelf water and open ocean water can be difficult to distinguish from other mixing mechanisms, such as the exchange processes driven by tides or by wind and wave action. Thus shelf convection remains a poorly understood process.

The general view is that shelf convection occurs in three not necessarily sequential stages (e.g. Killworth 1983): a production of dense water on the shelf, an exchange between the semi-enclosed marginal seas and the surrounding ocean, and finally, the descent of the dense waters down the continental shelf. The lateral density gradient across the front separating the cold dense water from the surrounding ambient fluid will drive a current along the front, as Coates et al. (1995) have demonstrated in their laboratory modelling of open ocean convection. They showed that this so-called rim current is crucial in the evolution of the mixed layer since, as it goes unstable, it generates a field of baroclinic eddies which promote a lateral exchange between the convecting region and the surrounding ambient fluid. This exchange disrupts and indeed can arrest the convective deepening. In shelf convection, the presence of the coastline and its irregular topographic features within the convecting region may locally break the geostrophic constraints near the coast, and influence the dynamics in the con-



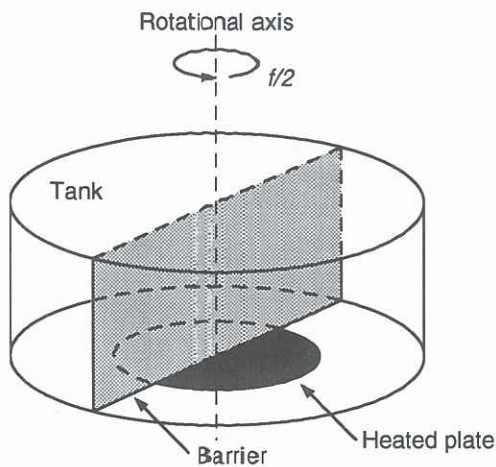


Figure 1: A sketch (not to scale) showing the geometry of the heated plate and the radial barrier.

vecting region.

In a laboratory study of an initially homogeneous ocean, Whitehead (1993) demonstrated that there was a complicated quasi-steady state exchange between the shelf and offshore waters when the shelf was subject to surface cooling, and obtained estimates of the heat transfer and temperature changes expected for a given surface cooling rate. Gawarkiewicz and Chapman (1995) have recently performed a numerical simulation in a homogeneous ocean subject to a negative buoyancy flux imposed on a half-elliptical surface region adjacent to the coast. Over the parameter range investigated, their simulations illustrated that a rim current does form and is subject to a similar baroclinic instability and eddy formation observed in the open ocean laboratory model of Coates et al. (1995). In this study, we report some preliminary experiments which extend these studies by examining the early evolution of the flow field in an initially stratified fluid.

## THE EXPERIMENT

The experiments were performed in the 1m diameter rotating tank described by Ivey et al. (1995) in which the convection is established by heating a centrally mounted 0.4m diameter plate built into the base of the tank. In this study we model the effect of a coastline by adding a vertical radial barrier across the centre of the heated plate (see fig. 1), thereby creating a semi-circular convection region adjacent to the model coastline. Temperature versus depth profiles at various radii along the radial barrier were measured by profiling a rack of fast response thermistors, while qualitative and quantitative measurements of the flow field were obtained by LIF (laser induced fluorescence) and PIV (particle image velocimetry, Stevens and Coates, 1994) respectively. For the present experiments, a horizontal light sheet was used in both techniques. The resolution requirements of PIV limited the field of view to span approximately 300 mm.

Run	$f$	$B$	$N$	$L_R$	Vis.
1	0.42	$1.46 \times 10^{-6}$	0.28	0.022	PIV
2	0.42	$2.47 \times 10^{-6}$	0.27	0.029	LIF
3	0.14	$2.02 \times 10^{-6}$	0.30	0.136	LIF

Table 1: A summary of the experimental parameters, where  $f$  is the Coriolis parameter [ $\text{rad s}^{-1}$ ],  $B$  is the buoyancy flux [ $\text{m}^2\text{s}^{-3}$ ],  $N$  is the buoyancy frequency [ $\text{s}^{-1}$ ], and  $L_R$  is the Rossby radius [m].

The experimental procedure was to initially fill the tank with the upper warm layer, at the ambient laboratory temperature to minimize heat loss, and then successively insert the cooler layers from below while the table was rotating. This method resulted in an almost linear initial stratification, as determined by the initial temperature profile. The fluid was allowed to come to solid body rotation before the experiment was initiated, and the temperature profiles and video recording commenced.

## RESULTS

### Rim current development

Three experiments have been conducted in which stratified fluids have been used. The experimental parameters are summarized in table 1.

On the initiation of the heating, a convecting mixed layer forms above the heated plate and begins to erode the overlying stratification. Initially, the mixed layer is confined above the plate, since the rotation acts to constrain any radial adjustment and Ivey et al. (1995) showed that, in this case, the depth  $h$  of the mixed layer was simply given by

$$h = 2^{1/2} B^{1/2} t^{1/2} / N \quad (1)$$

where  $B$  is the buoyancy flux,  $t$  is the elapsed time from the start of heating, and  $N$  is the buoyancy frequency. Eq. 1 continues to remain valid during the early stages in the growth of the instability, but eventually, the lateral transport by the instability will disrupt the convective deepening. Ivey et al. (1995) showed that this occurs by about  $9T$ , where  $T$  is the rotational period, in agreement with a theoretical prediction recently proposed by Visbeck et al. (1995).

Figure 2 shows the velocity vectors obtained near the top of the mixed layer during the evolution of the flow. The tank rotation in these runs is in the Northern Hemisphere (anti-clockwise) direction. The tops of the convective plumes which are forming above the heated plate can be seen in fig. 2 at  $0.33T$ , but even at this early time, an anti-cyclonic rim current can be seen to be flowing around the rim of the plate. Near the wall, however, the rim current does not exist and thus there must be some form of inflow to balance the fluid transport away from the wall in the rim current. Such inflow from the surrounding ambient fluid is visible in fig. 2, principally in the region adjacent to the wall (the upper left corner of fig. 2), although some inflow can still be seen along most of the visible rim.

Coates et al. (1995) showed in the absence of topographic effects, the magnitude of the rim current can



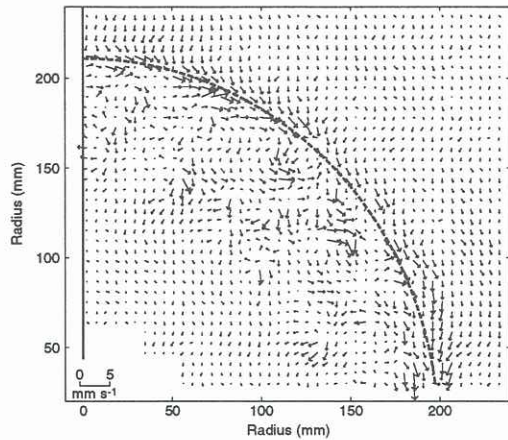


Figure 2: The early velocities for run 1 at  $t = 0.33T$ , near the top ( $0.83h$ ) of the mixed layer. The rim of the heated plate is marked by the dashed line and the radial wall by the solid line. The tank is rotating in the Northern Hemisphere (anti-clockwise) direction.

be predicted from the simple thermal wind balance and is

$$u_\theta \sim (Bt)^{1/2}, \quad (2)$$

where  $u_\theta$  is the tangential component of the velocity. Fig. 3 shows the rim current magnitudes  $u_\theta$ , normalized by  $(Bt)^{1/2}$ , as a function of the depth  $z$ , normalized by the depth  $h(t)$  of the mixed layer at the time each velocity measurement was made. Experimental results without the barrier (Coates et al. 1995) are also shown for comparison. Considering the difficulties in measuring the rim current as it goes unstable, the agreement between the two is good and suggests that the thermal wind balance continues to hold away from the barrier. We discuss how far away in the next section.

#### Rim current instability

Linear instability theory (Eady 1949, Samelson 1993) predicts that, in the absence of topographic effects, the rim current will go baroclinically unstable, and that the wavelength  $\lambda$  of the fastest growing mode will be a multiple of the Rossby radius  $L_R$ , defined by  $L_R = Nh/f$ . Experiments (Coates et al. 1995) have shown that the relationship is

$$\lambda = (3.3 \pm 0.6)L_R \quad (3)$$

but with the additional constraint that only an integral number of wavelengths can form around the rim.

The LIF image in fig. 4a, taken near the top of the mixed layer at  $4.0T$  for run 2, shows rather spectacularly that the baroclinic instability still forms even with the barrier present, although eddies appear to begin only about  $40^\circ$  or so around the perimeter from the barrier. This suggests that the barrier influences the flow out to about  $4.5L_R$ , beyond which the rim current can evolve without constraint, but considering the difficulty in determining precisely where the instability begins, this distance is also consistent with the instability wavelength  $\lambda \approx 3.3L_R$  from (3).

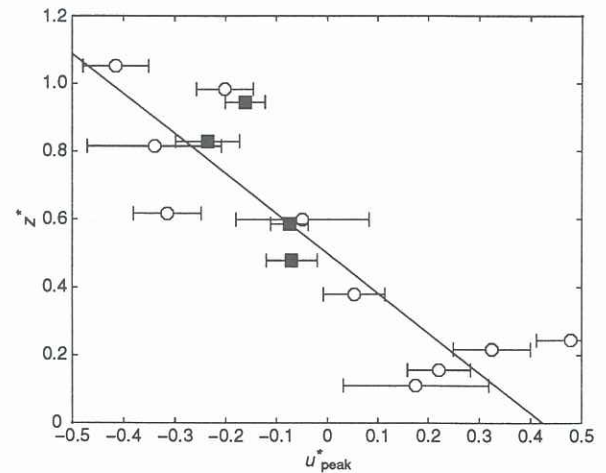


Figure 3: The peak non-dimensional rim current  $u_\theta^*$  plotted against the non-dimensional height  $z^*$ . The present data (run 1) are the solid symbols (■), while the data of Coates et al. (1995) appear as the open symbols (○). Their line of best fit is also shown.

While we do not have the data to further refine this value, we can say that provided  $L_R < \bar{W}$ , where  $\bar{W}$  is the mean or effective shelf width, we expect to see a rim current and its instabilities. The natural geometric length scale to use for  $\bar{W}$  appears to be the hydraulic radius (area/perimeter), since we do not have a constant shelf width in this problem. From fig. 4a, the instability wavelength is measured to be  $85 \pm 7$  mm, in good agreement with the value of  $96 \pm 17$  mm predicted by (3) without topographic effects, and suggests that in this region the dynamics are indeed uninfluenced by the barrier.

On the other hand, if the Rossby radius becomes of the same order as  $\bar{W}$ , then it would be expected that the dynamics of the flow would be quite different. Such a situation is illustrated in fig. 4b, taken from run 3 at  $3.44T$ , near the top of the mixed layer. A current is still present in this run, but it does not go unstable. The eddies which appear around the rim in fig. 4b are related to the convective plumes rising of the heated plate. (The eddy size is about twice the characteristic length scale of the turbulence.)

#### SUMMARY

The sequence of events observed in these preliminary laboratory experiments in a stratified fluid are similar to those observed in the numerical simulations of Gawarkiewicz and Chapman (1995). These simulations were performed in a homogeneous ocean with a gently sloping shelf, and subject to a negative buoyancy flux imposed on a half-elliptical surface region adjacent to the coast. The simulations were run with  $\bar{W}/L_R \approx 6$ , even greater than our run 2, and they reported the same three phases of the flow development observed in our current experiments. Firstly, there is a geostrophic adjustment, leading to the development of the rim current. The magnitude of this current in both the numerical simulations and in the current experiments agrees with earlier results obtained in the absence of the coastline. Secondly, the rim cur-



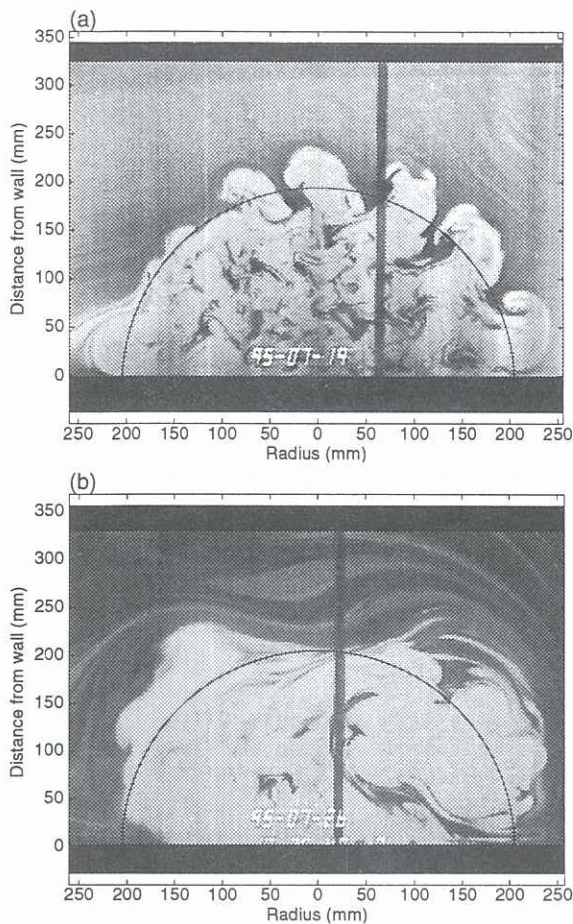


Figure 4: Overhead LIF images showing the development of the baroclinic instability in (a) run 2 at  $4.00T$  with the horizontal light sheet positioned at the height  $0.6h$ , and (b) run 3 at  $3.44T$  with the light sheet at  $0.8h$ . The rim of the heated plate is marked in both images.

rent becomes unstable and eddies are generated. The general shape and structure of the instabilities in the simulations are very similar to those observed in our experiments, but their instability wavelength is a little larger at  $\lambda \sim 5L_R$ . Finally, the last stage is the transport of fluid by the eddies.

The results, summarized in table 2, suggest that the ratio of the shelf width to the Rossby radius is a crucial parameter in the dynamics of the flow. If  $\bar{W}/L_R > 1$ , the rim current will go unstable and the eddies which form will be a major mechanism in the offshelf transport. If however  $\bar{W}/L_R < 1$ , the formation of the eddies is suppressed, as might be expected, with major consequences for the exchange mechanisms between shelf and surrounding seas.

**Acknowledgements:** This work was funded by the Australian Research Council and forms Environmental Dynamics Reference ED-1019-MC. Our thanks to Jeff Sturman and Chari Pattiaratchi for comments on the manuscript.

## REFERENCES

Coates, M. J., Ivey, G. N., and Taylor, J. R., 1995,

Run	$f$	$L_R$	$\bar{W}/L_R$
1	0.42	0.022	4.7
2	0.42	0.029	3.5
3	0.14	0.136	0.8
Simulation	$1.3 \times 10^{-4}$	840	6.0

Table 2: A comparison of the Rossby radius  $L_R$  with the mean shelf width  $\bar{W} = R/2$ , where  $R$  is the radius of the heated plate, in the present experiments and in the simulation of Gawarkiewicz and Chapman (1995). One difficulty in determining  $L_R$  is that the mixed layer depth  $h$  (and thus  $L_R$ ) grows in time, but as the  $e$ -folding time for the fastest growing wavelength is approximately  $1T$  (Samelson, 1993), we use the depth of the mixed layer at this time in computing  $L_R$ . The same time is used in computing the simulation  $L_R$ .

“Convectively driven mixed layer deepening in a rotating, stratified fluid: modelling deep ocean convection”, In press, *J. Phys. Oceanogr.*

Eady, E., 1949, “Long waves and cyclone waves”, *Tellus*, Vol. 1, pp. 33–52.

Gawarkiewicz, G., and Chapman, D. C., 1995, “A numerical study of dense water formation and transport on a shallow, sloping continental shelf”, *J. Geophys. Res.*, Vol. 100, pp. 4489–4507.

Hay, W. W., 1993, “The role of polar deep water formation in global climate change”, *Ann. Rev. Earth Planet. Sci.*, Vol. 21, pp. 227–254.

Huthnance, J. M., 1994, “Physical processes at the shelf edge”, Submitted to *Progress in Phys. Oceanogr.*

Ivey, G. N., Taylor, J. R., and Coates, M. J., 1995, “Convectively driven mixed layer growth in a rotating, stratified fluid”, *Deep Sea Res.*, Vol. 42, pp. 331–349.

Killworth, P. D., 1983, “Deep convection in the world ocean”, *Rev. Geophys. Space Phys.*, Vol. 21, pp. 1–26.

Price, J. F., and Baringer, M., 1994, “Outflows and deep water production by marginal seas”, *Progress in Phys. Oceanogr.*, Vol. 33, pp. 161–200.

Samelson, R. M., 1993, “Linear instability of a mixed-layer front”, *J. Geophys. Res.*, Vol. 98, pp. 10195–10204.

Stevens, C. L., and Coates, M. J., 1994, “Applications of a maximised cross-correlation technique for resolving velocity fields in laboratory experiments”, *J. Hydraul. Res.*, Vol. 32, pp. 195–212.

Visbeck, M., Marshall, J., and Jones, H., 1995, “On the dynamics of convective “chimneys” in the ocean”, Submitted to *J. Phys. Oceanogr.*

Walsh, J. J., 1991, “Importance of continental margins in the marine biogeochemical cycling of carbon and nitrogen”, *Nature*, Vol. 350, pp. 53–55.

Warren, B. A., 1981, “Deep circulation in the world ocean”, In *Evolution of Physical Oceanography*, B. A. Warren and C. Wunsch (eds).

Whitehead, J. A., 1993, “A laboratory model of cooling over the continental shelf”, *J. Phys. Oceanogr.*, Vol. 23, pp. 2412–2427.